

Mixed Convection Flow and Heat Transfer Behavior inside a Vented Enclosure in the Presence of Heat Generating Obstacle

M. U. Ahammad¹⁻³, M. M. Rahman², and M. L. Rahman³

¹Department of Mathematics, Dhaka University of Engineering and Technology (DUET),
Gazipur-1700, Bangladesh

²Department of Mathematics, Bangladesh University of Engineering and Technology (BUET),
Dhaka-1000, Bangladesh

³Department of Mathematics, Rajshahi University,
Rajshahi-6205, Bangladesh

Copyright © 2013 ISSR Journals. This is an open access article distributed under the *Creative Commons Attribution License*, which permits unrestricted use, distribution, and reproduction in any medium, provided the original work is properly cited.

ABSTRACT: A numerical investigation has been carried out for an MHD mixed convection problem to realize the influence of solid fluid thermal conductivity ratio as well as diameter of the centered obstacle on the flow and thermal fields in a ventilated cavity. The basis of the current paper is the numerical solutions of the Navier-Stokes equation along with the energy equation, wherein Galerkin weighted residual finite element technique is adopted with the help of Newton–Raphson iterative algorithm. The computation is performed for a wide range of relevant parameters such as thermal conductivity ratio between solid and fluid K (0.2 – 50), diameter of the inner block D (0.1 – 0.7) and Richardson number Ri (0.1 – 10). The streamlines and isotherms have been used for the visualization of the fluid flow structure and thermal field characteristics. Moreover, the findings of this analysis are also displayed by the average Nusselt number on the heated surface and average fluid temperature in the cavity. The study concludes that a small sized block and a lower value of thermal conductivity ratio is more effective for heat transfer phenomenon of the enclosure.

KEYWORDS: Heat transfer, heat generation, mixed convection, solid block, vented enclosure.

1 INTRODUCTION

Combined free and forced convection flow and heat transfer in an enclosure has many significant engineering, technological and natural applications. This includes nuclear reactors, heat rejection systems, heat exchangers, solar energy storage, refrigeration devices, lubrication technologies and cooling of electronic systems.

Many numerical and experimental studies have been performed on the mixed convection in the cavity. Costa and Raimundo [1] analyzed the problem of steady mixed convection in a square enclosure with a rotating circular cylinder where the enclosure was considered differentially heated. The effect of mixed convection in a partially divided rectangular enclosure was carried out by Hsu and How [2]. Manca et al. [3] experimentally performed mixed convection for the assisting forced flow configuration in a channel with an open cavity. They reported that for a large Reynolds number ($Re = 1000$), two nearly distinct fluid motions such as parallel forced flow in the channel and recirculation flow inside the cavity were found. Raji and Hasnaoui [4] analyzed the mixed convection in ventilated cavities for opposing and assisting flows. In their work, the horizontal top wall and the vertical left wall were arranged with equal heat fluxes. Gau and Sharif [5] investigated combined forced and free convection in rectangular cavities with various aspect ratios considering moving isothermal side walls and a constant-flux heat source on the bottom wall. Mixed convection flow inside a ventilated cavity along with a centered heat conducting horizontal circular cylinder was presented by Billah et al. [6]. A numerical study was carried out by Shuja et al. [7]

for mixed convection in a square cavity due to heat generating rectangular body effect of outlet port positions. Rahman et al. [9] studied mixed convection in a rectangular cavity having a heat-conducting horizontal circular cylinder using finite element technique For a wide range of Rayleigh number ($10^3 \leq Ra \leq 10^6$), Kumar and Dalal [10] conducted natural convection in an enclosure with a heated square cylinder. They focused that the uniform wall temperature heating is significantly unlike from the uniform wall heat flux heating. Rahman et al. [11] performed mixed convection in a ventilated square cavity with heat conducting solid circular cylinder placed horizontally. Chamkha [12] studied unsteady laminar mixed convection problem assuming the effect of magnetic field of electrically conducting and heat generating or absorbing fluid in a vertical lid-driven cavity. The fluid flow behavior of combined convection in lid-driven cavity containing a circular body was computed by Oztop et al. [13]. Oh et al. [14] performed a numerical analysis on the natural convection in a vertical square cavity keeping a temperature difference across the enclosure with a heat generating conducting body. The authors reported the variation of streamlines, isotherms and average Nusselt number for each Rayleigh number at the hot and cold walls with respect to temperature difference ratios. Prandtl number's effect on hydromagnetic mixed convection in a double-lid driven cavity confining a heat-generating obstacle have been investigated by Rahman et al. [15]. Ahammad et al [16] studied the performance of different inlet and outlet locations on the flow and heat transfer for the MHD mixed convection problem in a ventilated cavity containing a heat generating square block and they were established that flow and thermal fields have strong dependence on the position of inlet and outlet openings. Heat transfer characteristics of horizontal cylinder cooling under single impinging water jet was presented by Abo El-Nasr et al [17]. Veera Suneela Rani et al [18] performed the radiation effects on convective heat and mass transfer flow in a rectangular cavity. The combine influence of radiation and dissipation on the convective heat and mass transfer flow of a viscous fluid through a porous medium in a rectangular cavity using Darcy model was analyzed in their study.

In this paper, we focus attention on the flow and heat transfer characteristics inside a vented enclosure heated bottom wall in the presence of heat generating centered solid block for a two-dimensional steady laminar mixed convection problem.

2 GEOMETRY OF THE PROBLEM

The geometry of the present study is illustrated in Fig. 1. in which a Cartesian co-ordinate system is used with origin at the lower left corner of the working domain. It consists of a square enclosure of length L having a centered heat generating square solid block. The bottom wall of the cavity is subjected to hot with temperature T_h while the other sidewalls are kept insulated. The solid body with diameter d and a thermal conductivity of k_s generates uniform heat Q_0 per unit volume. The inflow opening is placed on the left bottom corner of the cavity while the outflow opening is on the right top corner as shown in the schematic and the size of each opening is $w = 0.1L$. A uniform magnetic field of strength B_0 is enforced in the horizontal direction on the right adiabatic wall. The incoming flow through the inlet is assumed at a uniform velocity u_i , ambient temperature T_i whereas the outgoing flow by the exit port is assumed to have zero diffusion flux for all variables and all solid boundaries are supposed to be rigid no-slip walls.

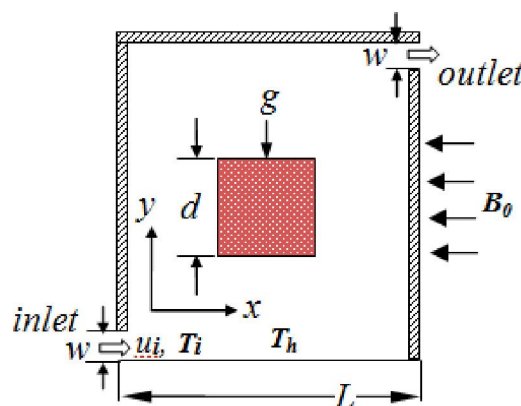


Fig. 1. Computational system

3 MATHEMATICAL MODELING AND SOLUTION PROCESS

The working fluid within the enclosure is supposed to be incompressible, Newtonian, two-dimensional, steady and laminar with all the fluid properties assumed as constant except for density variation. The radiation effect is negligible and the viscous dissipation is absent for the considered fluid. The governing equations for the problem under Boussinesq approximation can be described in vector forms as below:

$$\nabla \cdot \underline{q} = 0 \quad (1)$$

$$(\underline{q} \cdot \nabla) \underline{q} = -\frac{1}{\rho} \nabla p + \nu \nabla^2 \underline{q} + \underline{F} \quad (2)$$

$$(\underline{q} \cdot \nabla) T = \alpha \nabla^2 T \quad (3)$$

$$(\underline{q} \cdot \nabla) T_s + \frac{\rho c_p}{k_s} Q_0 = 0 \quad (4)$$

where it is taken that $F_x = 0$ and $F_y = g\beta(T - T_i) - \frac{\sigma B_0^2 v}{\rho}$

where \underline{q} is the velocity vector, \underline{F} is the body force, T and T_s denotes the temperature of the fluid and solid block, ν and α are the kinematics viscosity and the thermal diffusivity respectively; p is the pressure, ρ is the density, c_p is the specific heat at constant pressure k_s is the thermal conductivity of the solid block and Q_0 is the uniform constant heat flux.

The above equations are made dimensionless by introducing the following non-dimensional variables

$$X = \frac{x}{L}, Y = \frac{y}{L}, U = \frac{u}{u_i}, V = \frac{v}{u_i}, P = \frac{p}{\rho u_i^2}, \theta = \frac{(T - T_i)}{(T_h - T_i)}, \theta_s = \frac{(T_s - T_i)}{(T_h - T_i)}$$

Taking into account the aforesaid assumptions on the equations (1-4), the non-dimensional equations for the problem are given as follows:

$$\frac{\partial U}{\partial X} + \frac{\partial V}{\partial Y} = 0 \quad (5)$$

$$U \frac{\partial U}{\partial X} + V \frac{\partial U}{\partial Y} = -\frac{\partial P}{\partial X} + \frac{1}{Re} \left(\frac{\partial^2 U}{\partial X^2} + \frac{\partial^2 U}{\partial Y^2} \right) \quad (6)$$

$$U \frac{\partial V}{\partial X} + V \frac{\partial V}{\partial Y} = -\frac{\partial P}{\partial Y} + \frac{1}{Re} \left(\frac{\partial^2 V}{\partial X^2} + \frac{\partial^2 V}{\partial Y^2} \right) + \frac{Ra}{Re^2 Pr} \theta - \frac{Ha^2}{Re} V \quad (7)$$

$$U \frac{\partial \theta}{\partial X} + V \frac{\partial \theta}{\partial Y} = \frac{1}{Re Pr} \left(\frac{\partial^2 \theta}{\partial X^2} + \frac{\partial^2 \theta}{\partial Y^2} \right) \quad (8)$$

For solid obstacle the energy equation

$$\left(\frac{\partial^2 \theta_s}{\partial X^2} + \frac{\partial^2 \theta_s}{\partial Y^2} \right) + \frac{Re Pr}{K} Q = 0 \quad (9)$$

The dimensionless parameters appeared in the equations (6) - (9) are defined as follows

$$Re = u_i L / \nu, Ra = g \beta \Delta T L^3 / \nu \alpha, Pr = \nu / \alpha, Ri = Gr / Re^2, Ha = B_0 L \sqrt{\sigma / \mu},$$

$$Q = \frac{Q_0 L^2}{k_s \Delta T} \text{ and } K = k_s / k$$

where, Re , Ra , Pr , Ri , Ha , Q , and K stand for Reynolds number, Rayleigh number, Prandtl number, Richardson number, Hartmann number, heat generating parameter and solid fluid thermal conductivity ratio respectively. Also, $\Delta T = T_h - T_i$ and $\alpha = k / \rho c_p$ are respectively the temperature difference and thermal diffusivity of the fluid.

The appropriate non-dimensional boundary conditions for the present problem are:

$U = 1, V = 0, \vartheta = 0$ at the inlet.

Convective boundary condition (CBC), $P = 0$ at the exit.

$\vartheta = 1$ at the heated bottom wall.

$U = 0, V = 0, \frac{\partial \theta}{\partial N} = 0$ at all the adiabatic walls.

$\left(\frac{\partial \theta}{\partial N} \right)_{fluid} = K \left(\frac{\partial \theta_s}{\partial N} \right)_{solid}$ at the fluid- solid interfaces.

The average Nusselt number Nu at the hot surface is given by

$$Nu_{av} = - \int_0^1 (\partial \theta / \partial Y) dX$$

where as the bulk average fluid temperature inside the enclosure is

$$\theta_{av} = \int \theta d\bar{V} / \bar{V}, \text{ the volume of the enclosure is } \bar{V}.$$

The Galerkin weighted residual finite element scheme is used for the studied problem to solve the governing equations numerically. In this method, the continuum area of interest is discretized into finite element meshes, which are composed of irregular triangular elements. The coupled equations (5)-(9) are transformed into a system of integral equations using Galerkin weighted residual technique to reduce the continuum domain into discrete triangular domains. Then by imposition of boundary conditions the so obtained nonlinear algebraic equations are modified into a set of linear algebraic equations applying Newton-Raphson iteration technique. Last of all with the aid of triangular factorization method these linear equations are solved.

Grid Refinement Test and Code Validation

The details of grid refinement test and code validation for mixed convection problem with heat generating square block located at the center has been discussed in Ahammad et al. [16] and so is not repeated here.

4 RESULTS AND DISCUSSION

A numerical study is conducted herein to investigate the mixed convective two-dimensional laminar fluid flow along with thermal field characteristics considering the effect of thermal conductivity ratio K between solid and fluid as well as diameter D of the solid block. Governing parameters in this problem are the Reynolds number, Prandtl number, Hartmann number, and Richardson number. The value of Richardson number which is taken in the present work is 0.1, 1.0 and 10 to make simple the comparison process. Streamlines, isothermal lines, average Nusselt number at the hot wall and average fluid temperature inside the enclosure are used for the explanation of fluid flow and heat transfer manner.

Effect of Thermal Conductivity Ratio

Fig. 2. presents the streamlines for different values of K for the convective regimes of Ri (0.1, 1, 10) while $Re = 100, Ha = 10.0,$ and $Pr = 0.71$ are kept fixed. At $Ri = 0.1$ and $K = 0.2$ it is observed that the mainstreams capture almost the cavity and a counter-clockwise rotating cell develops just above the inlet openings. This is the reason that outer fresh and colder fluids which enters the cavity cannot come into intimate mixing with the inner hotter fluids. There is no disparity in the streamlines for the rest higher values of K . In the mixed convection domain ($Ri = 1$) for $K = 0.2$ it follows that the size of lower vortex increases and the top-left cornered open lines squeezes, as a result another anti-clockwise vortex appears occupying that region. But it can be noticed that with the increasing of thermal conductivity ratio the upper vortex reduces in size. A drastic change in flow lines is found at the higher value of $Ri = 10$. The main flow is found merely the right side of the obstacle and an extremely large vortex is created starting just above the inlet that spreads up to the top wall of the enclosure confining the obstacle.

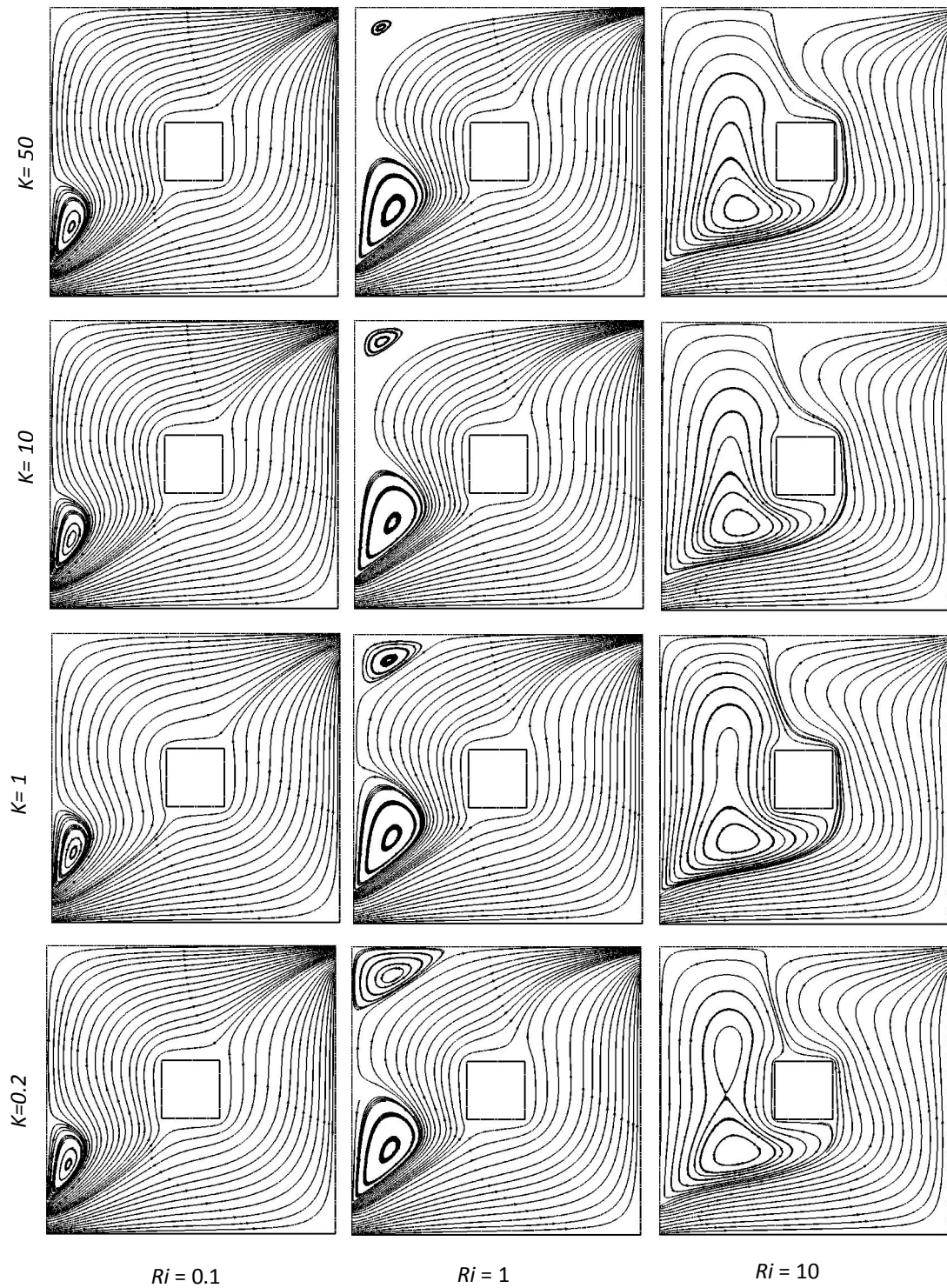


Fig. 2. Streamlines in a square ventilated cavity at different values of K , while $Re = 100$, $Ha = 10$, $Pr = 0.71$ and $Ri = 0.1, 1.0, 10$.

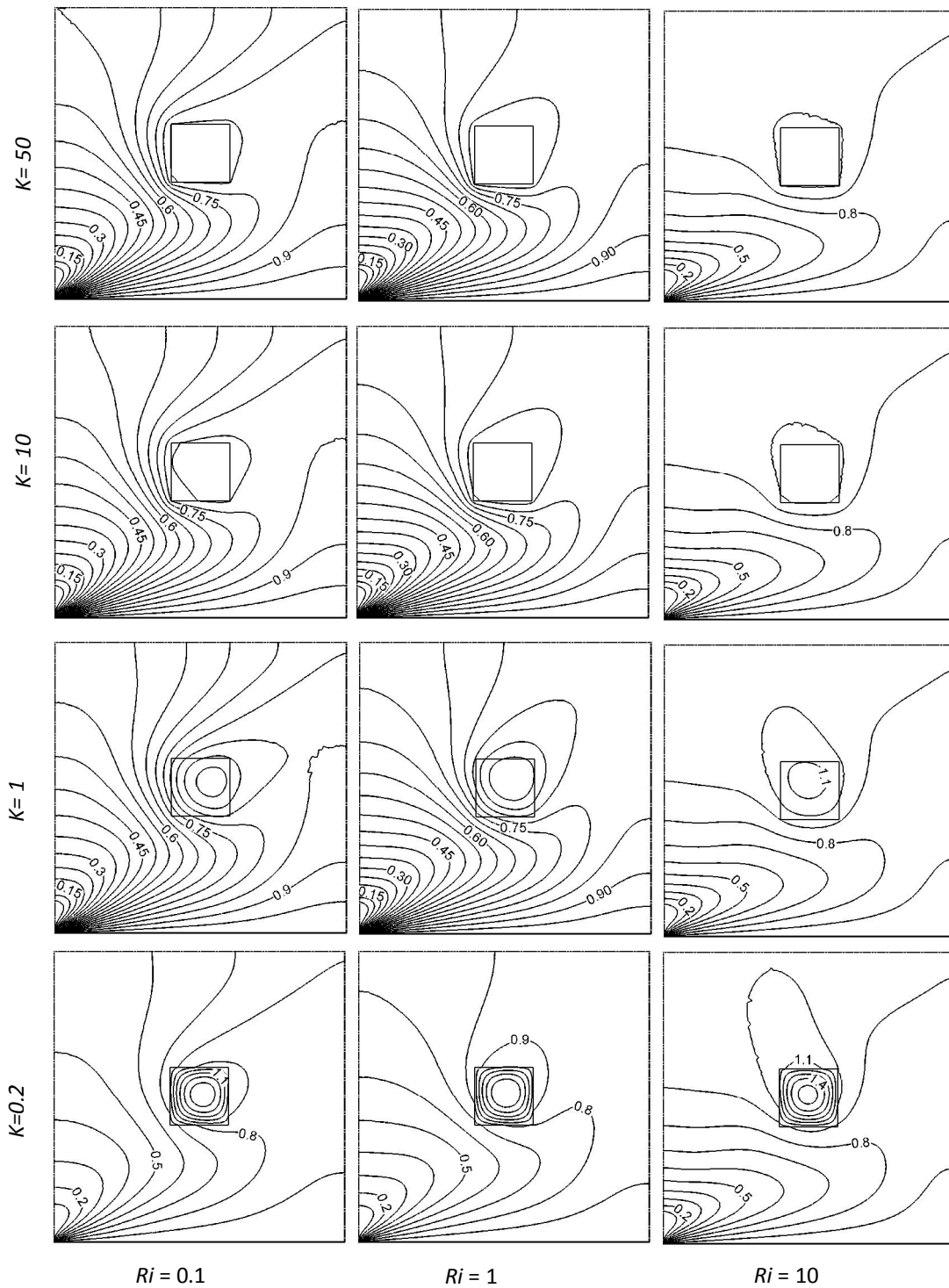


Fig. 3. Isotherms in a square ventilated cavity at different values of K , while $Re = 100$, $Ha = 10$, $Pr = 0.71$ and $Ri = 0.1, 1.0, 10$.

The corresponding isothermal lines for the chosen values of K in the range $0.1 \leq Ri \leq 10$ are displayed in Fig. 3. In the forced convection dominated region, highest circular thermal lines are distributed inside the centered solid block for the lowest value of $K = 0.2$. As the value of K increases from 0.2 to 1 it is noticed that the isotherms are dispersed all over the cavity and the compactness of heat lines inside the block reduces. It can be summarized that with increasing the value of K isothermal lines move out gradually from the solid obstacle and as a result it disappears at $K = 50$. With the comparison of $Ri = 0.1$, a minor change including right-top cornered plume shaped heat line is found in the patterns of isotherms at $Ri = 1$. For the free convection dominated region the behavior of temperature distribution changes markedly. The majority of isothermal lines are distributed below the heat generating block and plume shaped isotherm alters its direction from the right-top corner to left-top corner.

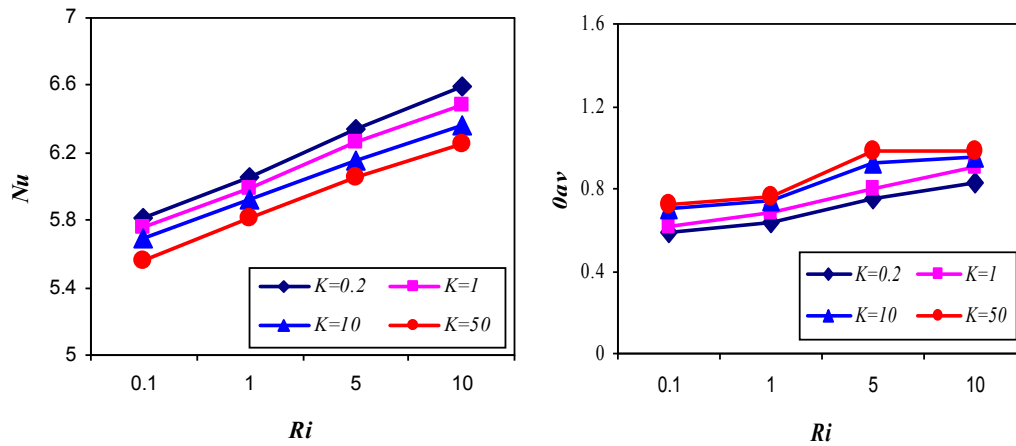


Fig. 4. Effect of thermal conductivity ratio K on average Nusselt number and average fluid temperature in the cavity while $Re = 100$, $Pr = 0.71$, $Ha = 10$, and $0.1 \leq Ri \leq 10$

In order to investigate the effect of thermal conductivity ratio K at solid fluid interface on heat transfer manner, average Nusselt number Nu at the bottom heated surface and average fluid temperature ϑ_{av} in the cavity are shown in Fig. 4. From this it can be observed that average Nusselt number enhances sharply as the value of K decreases and Ri increases. Therefore the rate of heat transfer is found optimum for the smallest value of K . On the other hand, ϑ_{av} increases for the rising value K and minimum average temperature is occurred when $K = 0.2$. Also for the lower values of K (0.2, 1) it is apparent that ϑ_{av} raises with the increasing value of all Ri but ϑ_{av} is seen about stationary in the domain $0.1 \leq Ri \leq 1$ and $5 \leq Ri \leq 10$ while it grows up in the area $1 \leq Ri \leq 5$ in the case of upper values $K=10$ and $K=50$.

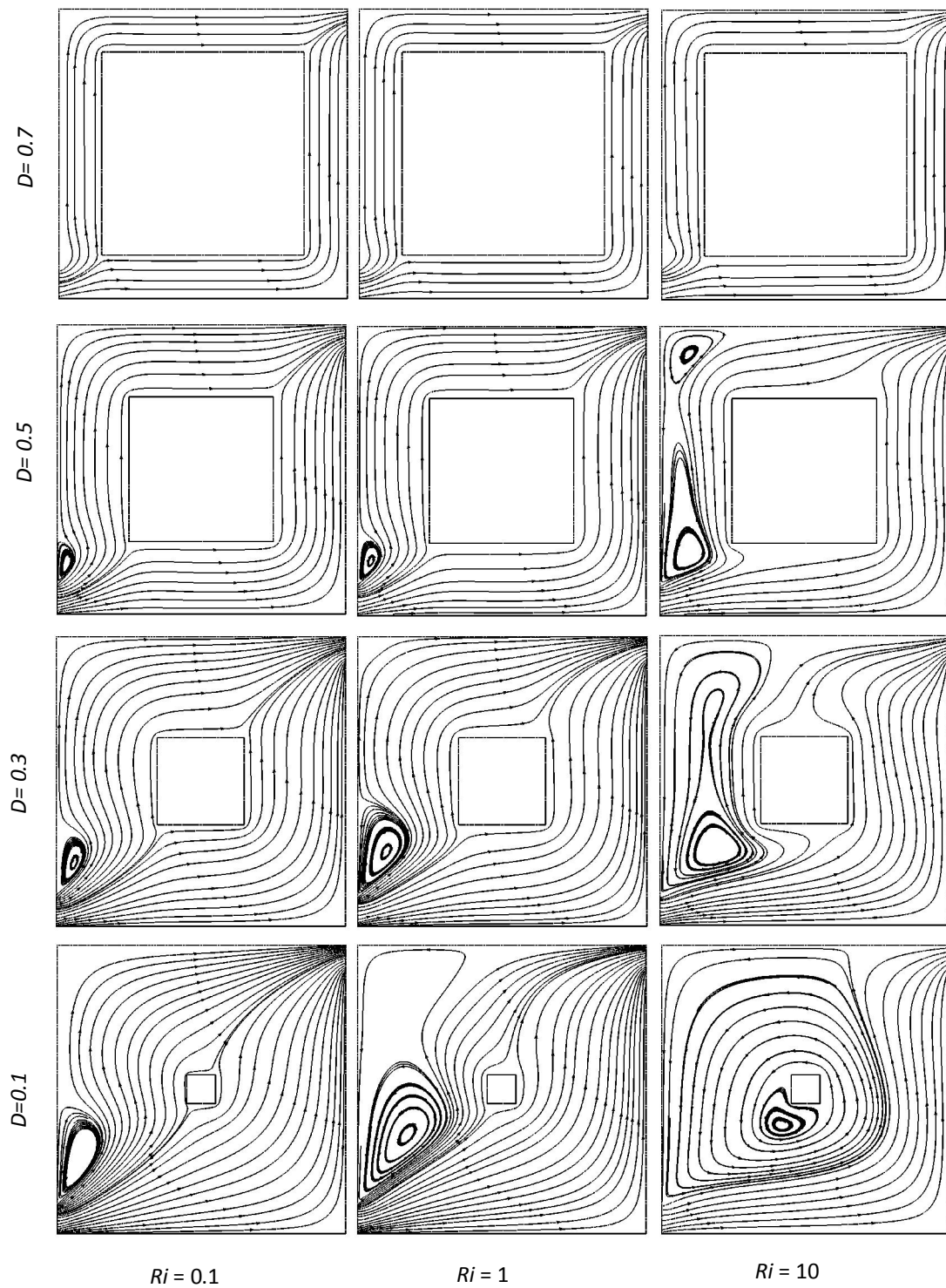


Fig. 5. Streamlines in a square ventilated cavity at different values of D , while $Re = 100$, $Ha = 10$, $Pr = 0.71$ and $Ri = 0.1, 1.0, 10$

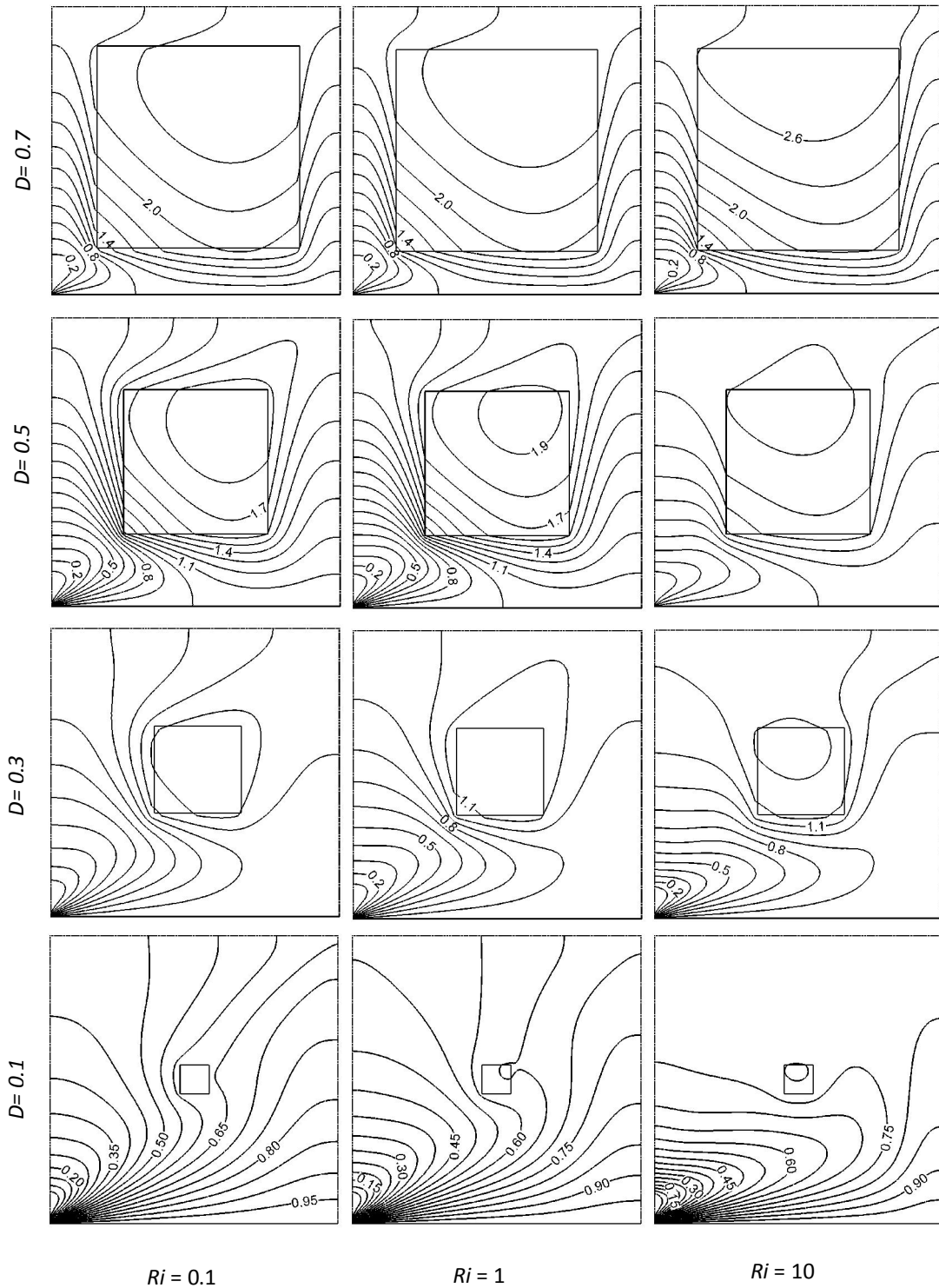


Fig. 6. Isotherms in a square ventilated cavity at different values of D , while $Re = 100$, $Ha = 10$, $Pr = 0.71$ and $Ri = 0.1, 1.0, 10$

Effect of Diameter of the Solid Block

The streamlines for different block size are depicts in Fig. 5. in the range of Richardson number $0.1 \leq Ri \leq 10$. At $Ri = 0.1$ and $D = 0.1$ the major streams stretched diagonally from the inlet to the exit opening and a recirculation cell is created just above the inlet of the cavity as expected. As the value of D increases the vortex becomes smaller and consequently it diminishes at the largest value of $D = 0.7$ due to the space availability in the cavity. Besides, streamlines are found to be nearly flat and vertical between the cavity and centered solid block for larger values of D ($= 0.5, 0.7$). In the pure mixed convection case ($Ri = 1$) the vortex expands rapidly at $D = 0.1$ and this recirculation cell sharply reduces and finally disappears for the maximum blocked size ($D = 0.7$) with the similar flow structures as seen at $Ri = 0.1$. One can easily be observed that for $D = 0.1$ the intensity of the vortex in the cavity increases too much and it captures the obstacle in the case of higher value of $Ri = 10$, this is happened since buoyancy effect increases. For $D = 0.3$ the counter-clockwise vortex shrinks from the right side and it vacates the block. A bi-cellular recirculation cell is created at $D = 0.5$ and it becomes narrow regarding $D = 0.1$ and $D = 0.3$. There is no change in flow patterns for $D = 0.7$ with the comparison of $Ri = 0.1$ and $Ri = 1$.

Fig. 6. illustrates the temperature distribution inside the vented enclosure for the four chosen value of block diameter D . For all the convective regimes of Richardson number Ri ($=0.1, 1, 10$) it is noticed that at $D = 0.1$ isotherms are concentrated near the inlet and a thermal boundary layer is formed in the vicinity of the bottom hot wall. The heat lines are scattered in the whole domain for the lower values of Ri ($=0.1, 1$) while for $D = 0.1$ these are seems to be curved below the heat generating block at $Ri = 10$. For higher values of D the heat lines are almost similar in all the selected range of Richardson number.

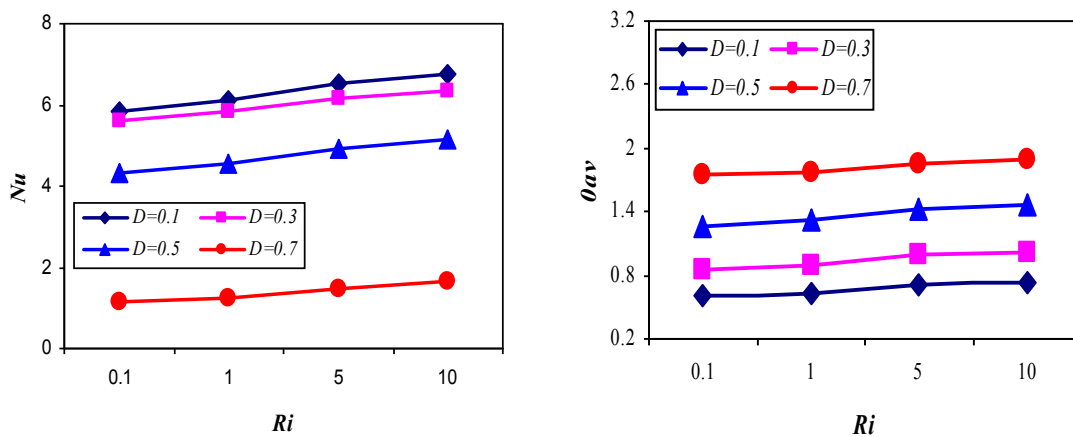


Fig. 7. Effect of solid block diameter D on average Nusselt number and average fluid temperature in the cavity while $Re = 100$, $Pr = 0.71$ $Ha = 10$ and $0.1 \leq Ri \leq 10$

5 CONCLUSION

Combined convection thermal along with flow field is analyzed numerically in a heat generating obstacle located in the ventilated enclosure. The considered pertinent parameters in this analysis are solid fluid thermal conductivity ratio and diameter of the obstacle with three convective regimes of Richardson number ($0.1, 1, 10$). The main conclusions that are drawn from the present article are as follows. (i) The highest heat transfer is recorded for the lowest value of K and it increases with increasing Ri . (ii) Lower thermal conductivity ratio shows the minimum average fluid temperature in the cavity. (iii) A small size of obstacle gives the maximum average Nusselt number. (iv) Average fluid temperature in the cavity is about independent of Ri and it is lowest for the smaller value of D .

REFERENCES

- [1] V. A. F. Costa and A. M. Raimundo, "Steady mixed convection in a differentially heated square enclosure with an active rotating circular cylinder," *International Journal of Heat and Mass Transfer*, vol. 53, pp. 1208–1219, 2010.
- [2] T.H. Hsu and S.P. How, "Mixed convection in a partially divided rectangular enclosure," *Numerical Heat Transfer, Part A*, vol. 31, pp. 655-683, 1997.
- [3] O. Manca, S. Nardini, and K. Vafai, "Experimental investigation of mixed convection in a channel with an open cavity," *Numerical Heat Transfer, Part A*, vol. 19, pp. 53-68, 2006.
- [4] A. Raji and M. Hasnaoui, "Mixed convection heat transfer in ventilated cavities with opposing and assisting flows," *International Journal Computer-Aided Engineering. Software*, vol. 17, no. 5, pp. 556–572, 2000.
- [5] G. Gau and M. A. R. Sharif, "Mixed convection in rectangular cavities at various aspect ratios with moving isothermal side walls and constant flux heat source on the bottom wall," *International Journal Thermal Science*, vol. 43, pp. 465–475, 2004.
- [6] M. M. Billah, M. M. Rahman, and M. A. Uddin, "Mixed convection inside a ventilated cavity along with a centered heat conducting horizontal circular cylinder," *Engineering e-Transaction*, vol. 6, no. 1, pp. 62–69, 2011.
- [7] S. Z. Shuja, B. S. Yilbas, and M.O. Iqbal, "Mixed convection in a square cavity due to heat generating rectangular body effect of cavity exit port locations," *International Journal of Numerical Methods for Heat and Fluid flow*, vol. 10, no. 8, pp. 824–841, 2000.
- [8] J.N. Reddy, *An Introduction to Finite Element Analysis*, McGraw-Hill, New-York, 1993.
- [9] M. M. Rahman, M. A. Alim, and M. A.H. Mamun, "Finite element analysis of mixed convection in a rectangular cavity with a heat-conducting horizontal circular cylinder," *Non-linear analysis: Modeling and Control*, vol. 14, no. 2, pp. 217–247, 2009.
- [10] A. Kumar De and A. Dalal, "A numerical study of natural convection around a square, horizontal, heated cylinder placed in an enclosure," *International journal Heat Mass Transfer*, vol. 49, pp. 4608-4623, 2006.
- [11] M. M. Rahman, M. Elias, and M. A. Alim, "Mixed convection flow in a rectangular ventilated cavity with a heat conducting square cylinder at the center," *Journal of Engineering and Applied Sciences*, vol. 4, no.5, pp. 20-29, 2009.
- [12] A. J. Chamkha, "Hydro magnetic combined convection flow in a vertical lid- driven cavity with internal heat generation or absorption," *Numerical Heat Transfer Part A*, vol. 41, pp. 529-546, 2002.
- [13] H. F. Oztop, Z. Zhao, and B. Yu, "Fluid flow due to combined convection in lid-driven enclosure having a circular body," *International journal Heat and Fluid Flow*, vol. 30, pp. 886–901, 2009.
- [14] J. Y. Oh, M. Y. Ha, and K. C. Kim, "Numerical study of heat transfer and flow of natural convection in an enclosure with a heat generating conducting body," *Numerical Heat Transfer, Part A*, vol. 31, pp. 289-304, 1997.
- [15] M. M. Rahman, R. Nasrin, and M. M. Billah, "Effect of Prandtl number on hydromagnetic mixed convection in a double-lid driven cavity with a heat-generating obstacle," *Engineering e-Transaction*, vol. 5, no. 2, pp. 90–96, 2010.
- [16] M.U. Ahammad, M.M. Rahman, and M.L. Rahman, "Effect of inlet and outlet position in a ventilated cavity with a heat generating square block," *Engineering e-Transaction*, vol. 7, no. 2, pp. 107–115, 2012.
- [17] M. M. Abo El-Nasr, M. A. Abidou, and H. A. Hussein, "Heat transfer characteristics of horizontal cylinder cooling under single impinging water jet," *International Journal of Applied Sciences and Engineering Research*, vol. 1, no. 2, pp. 287–301, 2012.
- [18] A. Veera Suneela Rani, Dr. V. Sugunamma, and N. Sandeep, "Radiation effects on convective heat and mass transfer flow in a rectangular cavity," *International Journal of Innovation and Applied Studies*, vol. 1, no. 1, pp. 118-152, 2012.

APPENDIX I. NOMENCLATURE

B_0	magnetic induction (Wb/m^2)
g	gravitational acceleration (ms^{-2})
Gr	Grashof number
h	convective heat transfer coefficient ($Wm^{-2}K^{-1}$)
Ha	Hartmann number
k	thermal conductivity of fluid ($Wm^{-1}K^{-1}$)
k_s	thermal conductivity of solid ($Wm^{-1}K^{-1}$)
K	solid fluid thermal conductivity ratio
L	length of the cavity (m)
Nu	Nusselt number
n	dimensional distances either x or y direction acting normal to the surface
N	non-dimensional distances either X or Y direction acting normal to the surface
p	dimensional pressure (Nm^{-2})
P	dimensionless pressure
Pr	Prandtl number
Ra	Rayleigh number
Re	Reynolds number
Ri	Richardson number
Q	non-dimensional heat-generating parameter
Q_0	uniform heat flux
T	dimensional temperature (K)
ΔT	dimensional temperature difference (K)
u, v	dimensional velocity components (ms^{-1})
U, V	dimensionless velocity components
\bar{V}	cavity volume (m^3)
w	height of the opening (m)
x, y	Cartesian co-ordinates (m)
X, Y	dimensionless Cartesian coordinates
<i>Greek symbols</i>	
α	thermal diffusivity (m^2s^{-1})
β	thermal expansion coefficient (K^{-1})
ν	kinematic viscosity (m^2s^{-1})
θ	non dimensional temperature
ρ	density of the fluid (kgm^{-3})
<i>Subscripts</i>	
av	average
h	heated wall
i	inlet state